ARTICLE NO. 77-854

Experimental Study of the Combustion Processes in Granular Propellant Beds

T. R. Davis* and K. K. Kuo†
The Pennsylvania State University, University Park, Pa.

Catastrophic failure of propulsion and gun systems has been attributed to abnormal combustion within granular propellant charges. The effects of igniter strength, propellant type, deterrent concentration, and projectile motion on the overall transient combustion processes in granular propellant beds were studied experimentally. The results show that igniter strength significantly affects the duration of the induction period and the accelerative behavior of the pressure front traveling through the bed; a weaker igniter causes a more pronounced pressure front acceleration. A large igniter volumé was found to reduce the rate of flame-spreading and pressurization processes. Combustion of slightly deterred propellants produced very rapid flame spreading, higher peak pressures, and higher pressurization rates than regularly deterred propellants. Propellant particle geometry was found to greatly affect the rate of total mass consumption within a propellant bed and thereby influence the peak pressures and pressure wave phenomena within the bed.

Introduction

THIS research was stimulated by the need for achieving deeper understanding of the ignition and flame-spreading phenomena in the combustion of granular solid propellants. The need for verification experiments has been the general consensus of participants in a recent JANNAF Workshop.[1] In addition to the need for establishing a data base in granular bed studies, the theoretical study of the combustion processes undertaken by the authors[2] requires a parallel experimental study to provide a direct means for verification of the theoretical model.

It is important to point out that there are a number of experimental investigations that are closely related to the present investigation. Squire and Devine[3] have recorded pressure-time traces at various locations along a short ($\simeq 2$ in.) granular bed; their data were compared with the results obtained from the Kuo, Vichnevetsky, and Summerfield[4] theoretical model in which the granular propellants are assumed to be fixed within the tightly packed bed. Bernecker and Price[5-7] have studied the transition from deflagration to detonation phenomena in granular explosives. Warlick[8] has conducted studies of shock-loading phenomena produced by the ignition process in naval guns. Soper[9] has also studied the grain velocities and pressure spikes occurring during ignition and flame spreading in naval gun systems. East and McClure[10] have photographed some transient flame-spreading phenomena in large-caliber guns. Other large-caliber experiments have been conducted by Horst et al.[11-13] Owing to the complicated ignition system associated with large-caliber systems, the experimental setup usually produces test results more complicated to model by a one-dimensional approach. Therefore, the experimental data may not be used conveniently for the verification of theoretical models based on one-dimensional assumption.

The work of Gerri et al.[14-16] and Alkidas et al.[17] is closer to the one-dimensional case because the granular bed is ignited at one end through a primer blast. Their chamber diameter is nearly the same as that used in the present investigation. However, it is important to point out the differences between these studies and those of the present investigation. In the work of Gerri et al.[14-16] the emphasis was placed on the length of the granular bed, and experiments were carried out using three different chamber lengths (5.8,10.84, and 20.16 cm). Other principal variables studied were the primer vent geometry and the shot start pressure simulated by varying the strength of the shear disk in the venting bomb. The work of Alkidas et al.[17] emphasizes the effects of propellant initial loading fraction, ullage space, and orientation of the chamber for various loading densities.

This paper, however, addresses the effects of primer strength, propellant type, deterrent concentration, and downstream boundary condition on the overall combustion process by systematic variation of these parameters. The overall research objectives of this experimental study are 1) to verify the theoretical model that parallels this study; 2) to improve the understanding of transient combustion in order to reduce hazards and improve the design of propulsion systems; 3) to provide the physical model and boundary conditions required in the solution of the theoretical model, and 4) to evaluate the effects that a single variable (i.e., igniter strength, propellant composition, or downstream boundary) has on the overall combustion process.

The phenomena that occur during the transient combustion event generally include: penetration of hot ignition gases into the granular bed, convective heating of the propellant to ignition, compaction of the granular bed, rapid pressurization within the combustion chamber, propagation of the peak pressure toward the downstream end of the chamber, flame spreading within the propellant bed, and rapid depressurization of the chamber following the rupture of a shear disk or motion of a projectile.

It is beyond the scope of this experimental effort to study these phenomena individually. Indeed, they are so interrelated that complete segregation of each process is virtually impossible. The purpose of this work is to describe the collective effect of these phenomena on the overall combustion process.

Experimental Setup

A schematic drawing of the experimental test rig is shown in Fig. 1. The main components are 1) the igniter chamber that houses the primer, 2) the main combustion chamber that

Presented as Paper 77-854 at the AIAA/SAE 13th Propulsion Conference, Orlando, Fla., July 11-13, 1977; submitted Aug. 10, 1977; revision received Feb. 20, 1979.

Index category: Combustion Stability, Ignition, and Detonation.

*Graduate student, Dept. of Mechanical Engineering; presently working at Bethlehem Steel Corporation, Bethlehem, Pa.

†Associate Professor, Dept. of Mechanical Engineering. Member AIAA.

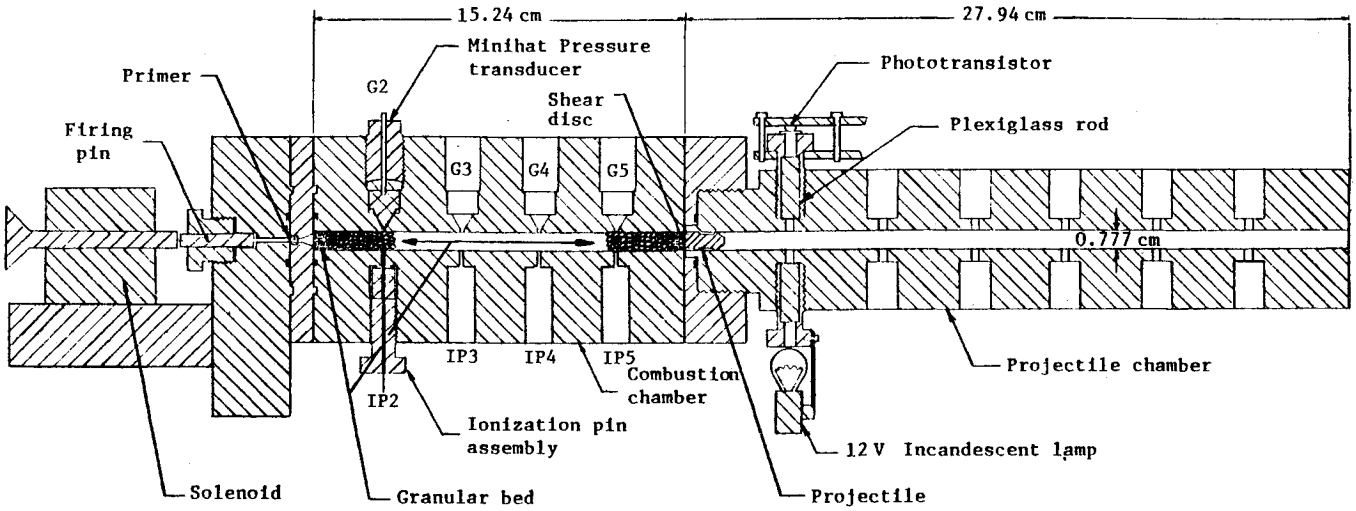

Fig. 1 Schematic drawing of the experimental test rig.

contains granular propellants, and 3) the projectile chamber. During the course of these experiments, three basic combustor assembly configurations were used: 1) gaseous ignition system with shear disk and shear disk retainer; 2) impact primer ignition system with shear disk and shear disk retainer, and 3) impact primer ignition system with projectile and projectile chamber.

The shear disk retainer is merely a shortened version of the projectile chamber. The thick-walled combustion chamber, which has a smooth center bore of 0.777 cm and a length of 15.24 cm, is fabricated from "Elastoff 44" steel. The combustion chamber houses four pressure transducers and four ionization probes, which are evenly distributed and spirally located along the length of the chamber. Each ionization pin is located diametrically opposite to a pressure transducer. The pressure transducers used were Minihat gauges,[18] which are resistance-type transducers with a pressure range of 6800 atm and a sensitivity of 1360 atm/Ω, nominal. The ionization pins are small (0.081 = cm o.d.) coaxial tubes with dielectric material separating the inner and outer conductors. The projectile chamber contains a light source-sensor system which provides six distinct position-time points for the displacement of the projectile during the combustion process.

A block diagram of the data acquisition system is shown in Fig. 2. The analog data are recorded on a high-speed magnetic tape recorder (Hewlett-Packard model 3924B). When the tape recorder is operated in the reproduce mode, its output is recorded by a Biomation 1015 Transient Waveform Digitizer. The Biomation unit provides four channel data storage and 1024-bit memory per channel, and is capable of a maximum real-time resolution of 10 μs. When operating in the maximum resolution mode, the time axis output of the Biomation is expanded by a factor of 10,000.

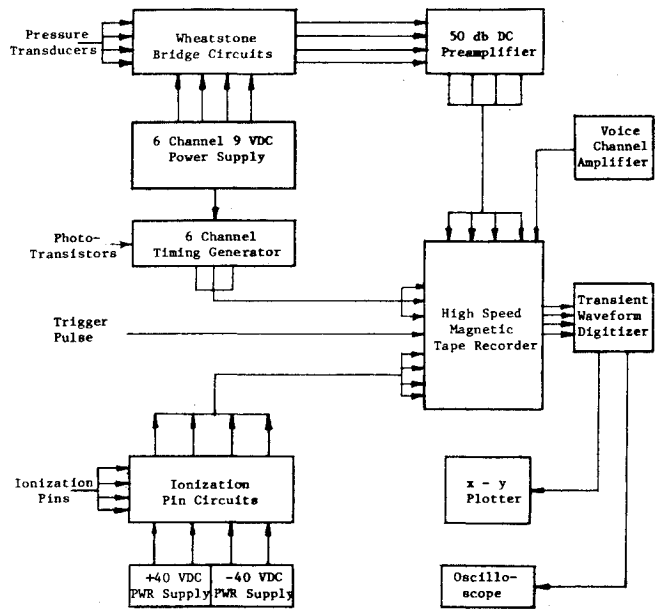

Fig. 2 Block diagram of the data acquisition system.

Discussion of Experimental Results

It is the purpose of this section first to present the experimental data obtained for a particular set of conditions that is called the baseline case. Using this as a basis, a qualitative explanation of the physical processes that occur during the rapid combustion event is given. Second, data for which a single variable has been changed from the baseline case are presented, and a direct comparison is made in order to study the effects of primer strength, propellant type, and boundary conditions.

Baseline Case

For convenience of comparison, a baseline case has been designated as a test firing with the following conditions: 1) WC-870 ball propellant (properties are listed in Table 1), 2) 7.00-g loading weight in a 30-caliber chamber, 15.24 cm long, 3) FA-34 percussion primer (constituents of the primer are listed in Table 2), and 4) 0.81-mm stainless steel shear disk at the downstream boundary.

The results for a typical test firing for the baseline case are shown in Fig. 3; the curves are offset vertically for clarity. Only three ionization pin traces are shown because IP 2 is discharged by igniter gases, and the discharge occurs almost simultaneously with the firing pin pulse. Since it does not give useful information about flame spreading, IP 2 was not used for most of the test firings. Several significant phenomena can be seen immediately:

1) The first discernible pressure rise for each pressure gauge occurs consecutively for G2 to G5, indicating the existence of a pressure wave traveling along the length of the chamber.

2) The pressurization rate increases consecutively for downstream positions.

3) The downstream gauges (G4, G5) indicate a second pressure peak, whereas the upstream gauges (G2, G3) show only a single peak.

4) The first discernible voltage on each IP trace occurs slightly before the first discernible pressure rise at each position.

Table 1 Physical, compositional, and thermochemical data of WC-870 and WC-846 propellant[19]

Particle shape	WC-870 Spherical	WC-846 Cylindrical disk
Granulation		
Max particle diam	0.0965 cm	0.0686 cm
Min particle diam	0.0686 cm	0.0406 cm
Web	...	0.0381 cm
Gravimetric density	0.960 g/cm^3	0.980 g/cm^3
% Nitroglycerin	10.0	10.0
% Nominal nitrogen		
Content of nitrocellulose	13.15	13.15
%Deterrent coating	5.2	4.9
Heat of explosion	870 cal/g	883 cal/g
Flame temperature	2831K	2858K

Table 2 Physical and compositional data of FA-34 and FA-41 primers[a,3,20]

Ingredient	% by weight	Density, g/cm^3
PETN	5.0±1	1.77
Lead styphnate	37.0±5	3.02
Tetracene	4.0±1	1.05
Aluminum powder	7.0±1	2.70
Antimony sulfide	15.0±2	4.12
Barium nitrate	32.0±5	3.24

[a]Average density of the mixture = 3.092 g/cm^3; weight of FA-34 primer ≅ 0.0358 g; weight of FA-41 primer ≅ 0.0224 g.

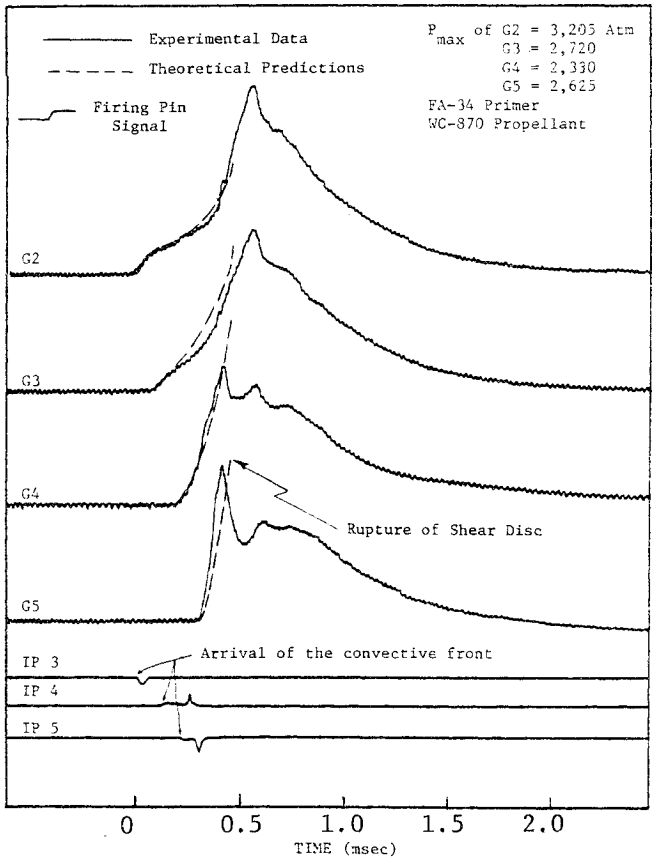

Fig. 3 Typical pressure-time and flame-spreading data for the baseline case (DAP Test No. 87).

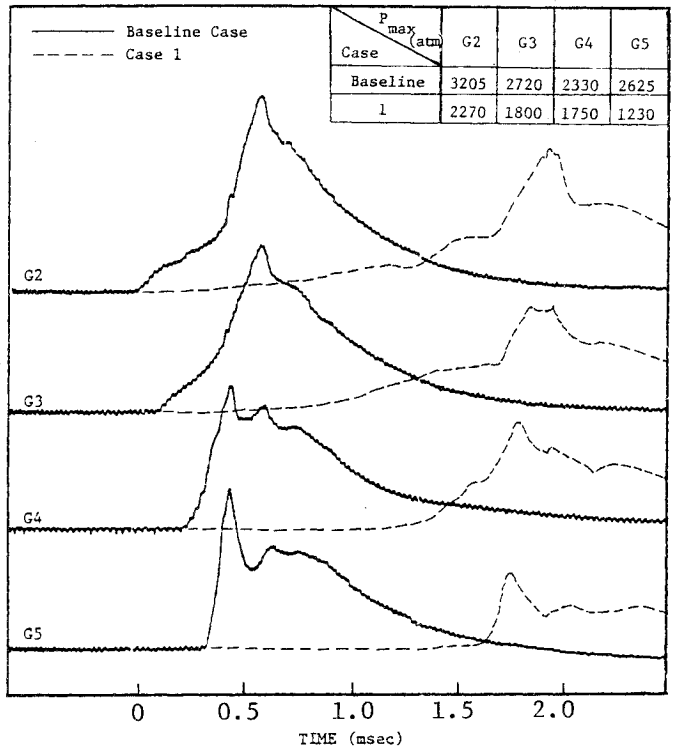

Fig. 4 Comparison of pressure-time traces between case 1 and the baseline case.

5) Before the shear disk ruptures, the pressure at the last gauge (G5) overtakes the pressure at the upstream locations.

6) All gauges depressurize in the later phase at approximately the same rate.

Some of these observations may be explained in the following manner. The time delay between the first discernible pressure rise of each gauge is due to the finite time period required for the penetration of the hot product gases into the interstitial voids, resulting in a finite rate of flame spreading through the granular bed. The increased pressurization rate for downstream positions can be understood by considering the sequence of pressure wave development through the granular bed. After the primer discharges into the combustion chamber, the upstream propellant grains ignite and begin to gasify, establishing a relatively weak pressure wave which travels in the downstream direction. Progressively, additional propellant grains begin to gasify, thus creating a higher pressure behind the pressure front. As the pressure level increases, the burning rate, and thus the rate of gasification, increases; this in turn results in even higher pressures. As the process continues, the pressure and the rate of gasification and pressurization continue to increase progressively, creating higher pressures and thus higher gasification rates. This "snowball' effect during the combustion of granular solid propellant is what causes the steep pressure gradient at the pressure wave front.

The second pressure peak experienced by the downstream gauges (G4, G5) is considered to be caused by the rupture of the shear disk. Upon rupturing, the subsequent forward motion of the shear disk establishes a rarefaction wave which travels backward through the chamber. This expansion wave causes an abrupt dip in pressure at the G5 and G4 locations, while the upstream gauges, G2 and G3, continue to show a smooth pressurization, since they are not affected by the rarefaction wave until later. G2 and G3 indicate an almost simultaneous peak pressure at the arrival of the rarefaction wave, since by this time the porosity in the upstream region has increased substantially because of particle motion and burning. The second pressure peaks, indicated by G4 and G5, are believed to be caused by compression waves that are generated in the region near the igniter and by the motion of burning particles toward the downstream portion of the bed.

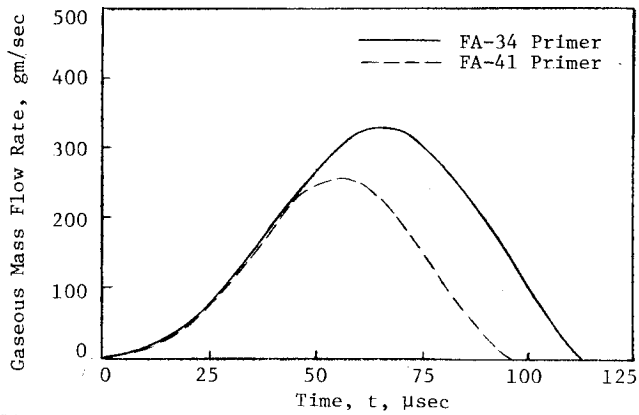

Fig. 5 Comparison of gaseous mass flow rates for FA-34 and FA-41 primers.

Since the ionization pins can be triggered by the ionized product gases, the measured ionization pin signals represent the arrival of the convective front of product gases. This front may not coincide with the ignition front of the granular propellants. In our opinion, the hot gas front is probably slightly ahead of the ignition front because the unburned propellants must be heated by the hot penetrating gases before an ignition condition is achieved. The ionization pin data indicate that the ionized product gases (or flame) arrive at downstream positions slightly ahead of the pressure front traveling through the bed. In Fig. 3, IP 4 and IP 5 consistently indicate a second pulse which occurs after the arrival of the steep pressure front. It is believed that this second pulse occurs when the pin is physically shorted to the wall of the chamber owing to the severe impact of the steep pressure wave. IP 3 consistently indicates a single pulse, since the pressure front is still relatively weak and is not able to crush or destroy the ionization pin as it does for downstream positions.

Before the shear disk ruptures, the pressure at the last gauge position, G5, overtakes the pressure at the upstream positions. This phenomenon occurs consistently in every test firing and is the result of the steep pressure gradient caused by the snowball effect described above. After the rupture of the shear disk, a significant quantity of unburned propellant is discharged from the downstream portion of the bed, resulting in a large void within the chamber. At this time all spatial dependence becomes negligible, as shown by the uniform depressurization of all gauges in the chamber. Downstream gauges exhibit a slightly more rapid depressurization due mainly to their proximity to the vented end of the combustion chamber.

To show a comparison between the theoretical predictions based on the Penn State Model[2] and experimental results, the predicted pressure-time traces for the baseline case at four gauge locations are superimposed on Fig. 3. The numerical calculations were terminated when the force acting on the shear disk reached a critical value. The comparison of the results at each gauge location shows a good agreement between theory and experiment in regard to both pressure front propagation velocity and pressurization rates.

Having defined the baseline case for this study and having explained the most significant phenomena, the purpose here is to alter a single variable of the baseline case and then observe any notable changes in the test results. The various cases tested are

Case 1: Gaseous H_2-O_2 igniter to replace FA-34 primer.
Case 2: FA-41 primer to replace FA-34 primer.
Case 3: WC-846 propellant to replace WC-870 propellant.
Case 4: Slightly deterred WC-846 propellant to replace WC-870 propellant.
Case 5: Projectile to replace the shear disk.

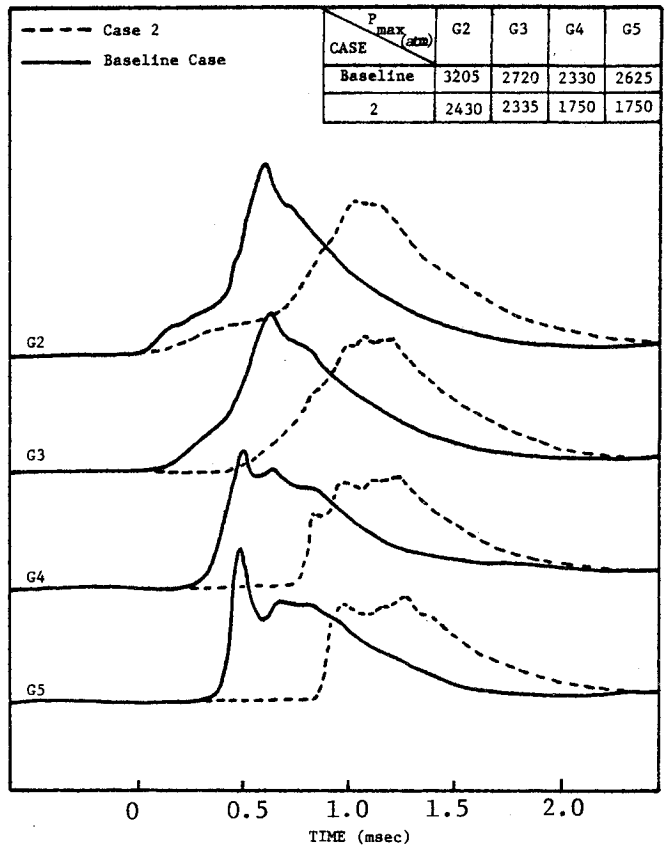

Fig. 6 Comparison of pressure-time traces between case 2 and the baseline case.

Case 1: Gaseous H_2-O_2 Igniter

The comparison of the pressure-time results of a typical case 1 test firing with the baseline case is given in Fig. 4. The general nature of the *p-t* traces in terms of the sequence of pressurization is similar to that of the baseline case. However, the rates of pressurization and flame spreading are much smaller than those of the baseline case. This is mainly due to the difference in igniter mass flow rate between the gaseous igniter and the FA-34 primer. Comparing the output of these two igniters, the maximum gaseous igniter mass flow rate of 18 g/s is reached in 0.60 ms from ignition, whereas the maximum primer mass flow rate of 327 g/s is reached in 0.065 ms. Since the gaseous igniter is a much weaker one than the FA-34 primer, it therefore produces a much slower combustion event in the granular bed.

In addition to the slower rate of ignition and combustion, the peak pressures for the case 1 configuration are lower than those in the baseline case. The reduced pressures for the case 1 configuration are most probably explained by the larger volume of the gaseous ignition system, which allows a reverse flow of product gases into the ignition chamber.[2] This increased volume (about 50% of the volume of the combustion chamber) is not available with the impact primer system. The reverse flow of hot product gases also results in a decrease in the amount of product gases available to heat the unburned (downstream) propellant to ignition. As a result, the convective mechanism described earlier is significantly attenuated; consequently, the combustion event requires a much longer period of time than the baseline case.

Case 2: FA-41 Primer

The chemical composition of the FA-41 impact primer is identical to that of the FA-34 primer, but physically it is approximately 63% of the mass. This smaller size results in a weaker ignition source with a smaller gaseous mass flow rate. The gaseous mass flow rates for FA-34 and FA-41 primers

were obtained through a primer characterization test procedure. A comparison of the mass flow rates from the two different primers is shown in Fig. 5. A comparison of the pressure-time traces of case 2 and the baseline case is given in Fig. 6 by starting the first discernible pressure rises at G2 at the same time. This clearly shows that the weaker primer produces slower burning and smaller pressure slopes than the baseline case during the initial phase of the combustion event (G2). Once the granular propellant is ignited, however, the pressure front accelerates at a much faster rate until the downstream gauges (G4 and G5) exhibit the same pressure slopes as the baseline case. The smaller igniter mass flow rate for the case 2 firing results in a lower rate of convective heat transfer during the initial stages of burning. This in turn decreases the initial rate of flame spreading within the bed, resulting in a decreased spatial variation of pressure along the chamber. In addition, the weaker primer does not compact the propellant bed as much as the stronger primer of the baseline case; less compaction results in more void volume in the downstream portion of the bed. Since the propellant particles are less tightly packed, there is less flow resistance within the bed. As a result, the acceleration of the pressure front becomes more pronounced.

Case 3: WC-846 Deterred Propellant

The properties of the WC-846 propellant are listed in Table 1. A comparison of the pressure-time data for case 3 and the baseline case is given in Fig. 7. The results of test firings for case 3 show a significant acceleration of the pressure front as it travels through the propellant bed. The peak pressures for case 3 are consistently higher than those of the baseline case. In evaluating these phenomena, it is important to consider the particle geometries. The WC-870 (baseline case) propellant is a spherical grain with a maximum diameter of 0.0965 cm and a loading weight in the 15.24-cm combustor of about 7.0 g. The WC-846 propellant has a cylindrical-disk shape with a maximum particle diameter of 0.0686 cm and a full loading weight approximately 9.0% greater than the baseline case. This difference in particle geometry has two significant effects on the initial state of the propellant bed: 1) the smaller WC-846 propellant results in a smaller initial porosity of the granular bed; and 2) the cylindrical-disk shape of the WC-846 grain offers a larger wetted propellant area per unit volume of the propellant particles.

The larger wetted surface area necessarily increases the total gasification rate of the propellant, thereby increasing the pressurization rate within the bed. In addition, the smaller porosity means a smaller void volume within the propellant bed and results in correspondingly higher peak pressures. In this comparison the authors concede that in changing the propellant type several variables have been altered from the baseline case; these include the variation of porosity, particle shape, and physico-chemical properties of the propellant. This complexity cannot be avoided unless special propellants are made for this purpose.

Case 4: Slightly Deterred WC-846 Propellant

In the theoretical modeling of combustion processes, one of the most difficult problems is that of accurately specifying the propellant deterrent concentration—a critical input to the computer solution of the model. Because the detailed distribution and thickness of deterrent coating on the particle grain is not accurately known, the propellant burning rate as a function of instantaneous particle radius cannot be calculated accurately. The objective here is to show the drastic changes in pressure-time data when the deterrent coating is reduced on the surface of the propellant grain, and to stress the need for concentrated studies in this area.

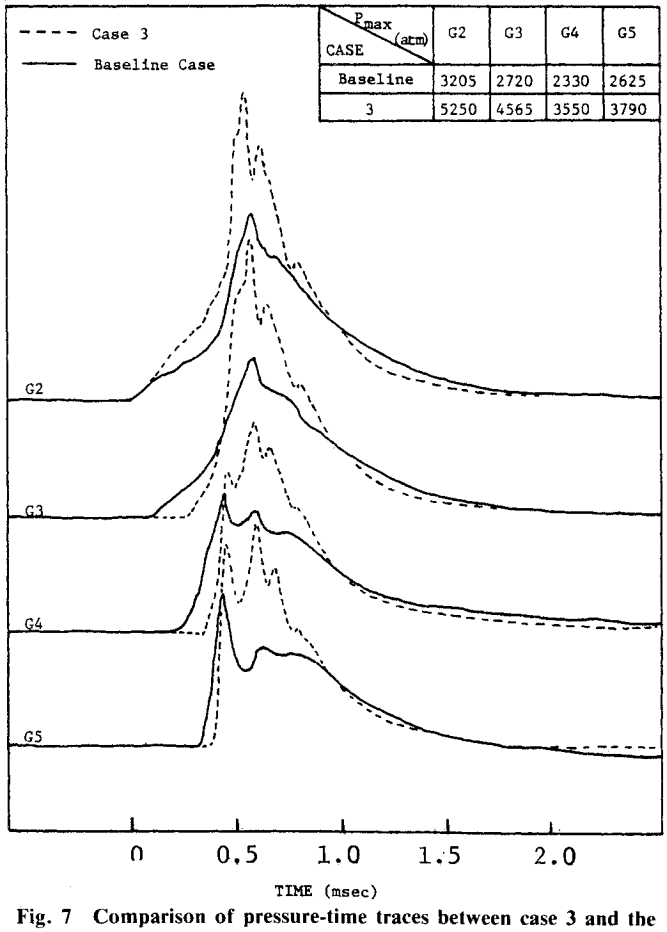

CASE \ P_{max} (atm)	G2	G3	G4	G5
Baseline	3205	2720	2330	2625
3	5250	4565	3550	3790

Fig. 7 Comparison of pressure-time traces between case 3 and the baseline case.

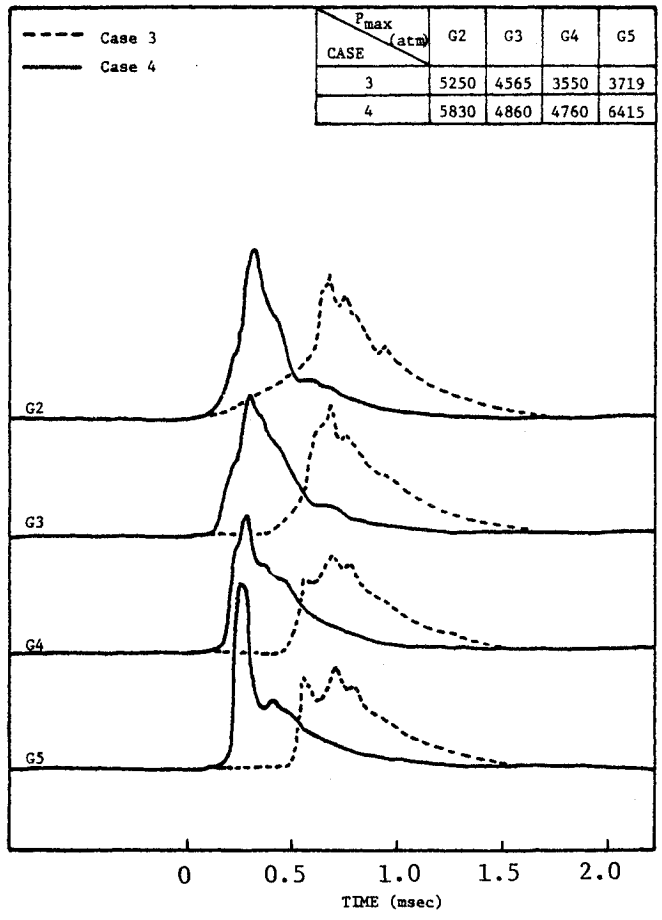

CASE \ P_{max} (atm)	G2	G3	G4	G5
3	5250	4565	3550	3719
4	5830	4860	4760	6415

Fig. 8 Comparison of pressure-time traces between case 3 and 4.

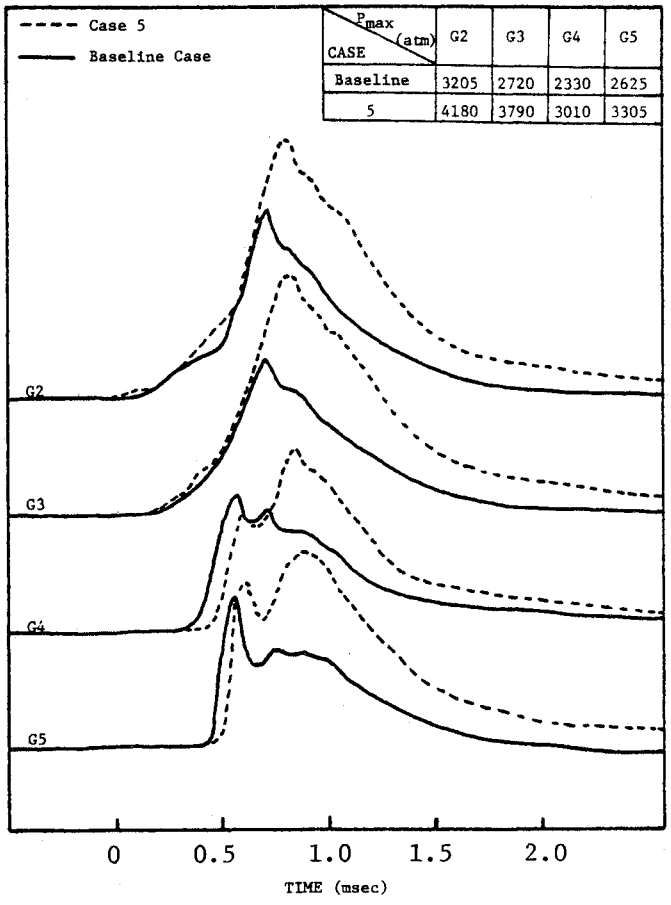

Fig. 9 Comparison of pressure-time traces between case 5 and the baseline case.

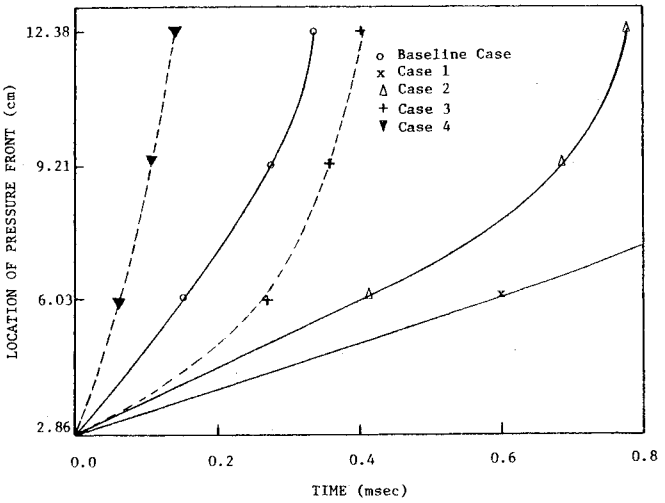

Fig. 10 Comparison of pressure front loci of various cases with the baseline case.

Figure 8 shows a comparison of the pressure-time histories for the 5% deterred (case 3) and the 0.54% slightly deterred (case 4) WC-846 propellant. This comparison shows that the burning characteristics for the slightly deterred propellant are significantly more energetic than those for the regularly deterred propellant. This can be seen by comparing the pressure slopes at the upstream gauge locations (G2, G3). Indeed, the pressure wave travels through the slightly deterred propellant bed in approximately 70 μs or six times faster than it travels through the regularly deterred propellants. The pressure levels for case 4 are significantly higher than for case 3, especially at the G5 position. This high pressure peak is probably due to the finite time required for the shear disk to rupture; since the pressure wave is so steep and moving so quickly, the rupture of the shear disk occurs at a much higher pressure than for the slower cases. As a result of the high pressure level, the rarefaction wave generated by the rupture of the shear disk is much more pronounced, causing a rapid depressurization at the G5 and G4 locations. Clearly, the percentage of deterrent content in the propellant grains can drastically affect the entire combustion process. To accurately model flame-spreading and combustion processes in a granular bed of deterred propellants, more accurate information about deterrent concentration distribution and propellant burning rate as a function of pressure and deterrent concentration is required.

Case 5: Moving Projectile as Downstream Boundary

In order to simulate a gun system more realistically, the venting shear disk at the downstream boundary was replaced by a projectile and a 27.94-cm gun barrel, as shown in Fig. 1. The shear disk remained in the new configuration (attached to the projectile) in order to permit a pressure buildup within the chamber before motion of the projectile. This setup provides a transient increase in volume of the the combustion chamber during the combustion event.

A comparison of case 5 and the baseline case is shown in Fig. 9. This direct comparison shows that the initial portion of both curves at each gauge location agrees closely. The effect of the projectile is most obvious after the shear disk has ruptured. Both cases indicate the effect of the rarefaction wave generated by the rupture and subsequent motion of the projectile (G4, G5). However, the case 5 data for G4 and G5 show a pronounced second peak, which is significantly higher than the first. The higher peak is caused by the continued gasification of propellant behind the projectile. The momentary dips in presure at G4 and G5 are not as great as that for the baseline case because of the inertia of the projectile. The projectile of case 5 accelerates less rapidly than the light shear disk of the baseline case, generating a less pronounced rarefaction wave that travels back through the bed. Since the projectile travels through the projectile chamber in approximately 0.5 ms, the case 5 combustion process is partially confined for that time period, resulting in a much slower pressure decay than that of baseline case.

The pressure wave development for the cases observed in this study can be summarized by considering the plots of pressure front loci shown in Fig. 10. Although the induction time for each case is different, for the purpose of this comparison the first discernible pressure rise at G2 for each case is designated as time equal to zero. The effect of igniter strength on the velocity of pressure front propagation through the bed can be seen by comparing the solid curves for cases 1 and 2 with the baseline case. The pressure front of case 1 propagates with the lowest velocity owing to the combination of a weak igniter and large gaseous igniter volume. Case 2 also has a weak output (FA-41), but because of the small primer volume the pressure front accelerates rapidly in the downstream portion of the granular bed. The baseline case combines a strong primer (FA-34) with a small primer volume to produce a relatively high-velocity pressure front.

The effect of propellent type on the propagation velocity of pressure front through the bed can be seen from the comparison of the dashed curves with the baseline case. For case 3 (WC-846) the velocity of the pressure front initially propagates with the lowest velocity owing primarily to a lower initial porosity of the granular bed. However it accelerates rapidly and eventually exceeds the velocity of the baseline case. For case 4 (slightly deterred WC-846) the velocity of the pressure front propagates with the highest velocity through the granular bed.

Conclusions

On the basis of the systematic variation of parameters in the test firings, several important conclusions of this investigation are summarized below:

1) The primer strength significantly affects the transient combustion processes in granular propellant beds. A weak primer, which causes less bed compaction, was found to have the following effects: a) a longer induction period before ignition of the bed and b) a pronounced pressure front acceleration.

2) Propellant deterrent concentration drastically affects the overall combustion and flame-spreading processes. Combustion of slightly deterred propellant was found to cause a) extremely rapid flame spreading due to rapid ignition of propellant particles and b) higher peak pressures due to higher gasification rates.

3) A larger propellant wetted surface area per unit volume combined with a higher loading density produces an increased rate of total mass consumption, resulting in more pronounced pressure wave phenomena within the granular propellant bed.

4) A moving downstream boundary produces the following effects, which are different from those of the vented chamber configuration: a) continued gasification of propellant behind the moving projectile, resulting in a maximum peak pressure after the projectile has started to move, and b) a longer time interval for the depressurization of the chamber.

Acknowledgments

This paper represents a part of the experimental results of the research work performed under Grants DAAG 29-74-G-0116 and DAAG 29-77-G-0163 at the Pennsylvania State University under the supervision of The Engineering Sciences Division of the U.S. Army Research Office at Research Triangle Park, N.C. The technical advice of N. J. Gerri of The Ballistic Research Laboratories and R. R. Bernecker of NSWC/WOL are greatly appreciated.

References

[1] Kuo, K. K., "A Summary of the JANNAF Workshop on: Theoretical Modeling and Experimental Measurements of the Combustion and Fluid Flow Processes in Gun Propellant Charges," CPIA Pub. 281, *13th JANNAF Combustion Meeting,* Vol. 1, Dec. 1976, pp. 213-233.

[2] Kuo, K. K., Koo, J. H., Davis, T. R., and Coates, G. R., "Transient Combustion in Mobile Gas-Permeable Propellants," *Acta Astronautica,* Vol. 3, 1976, pp. 573-591.

[3] Squire, W. H. and Devine, M. P., "The Interface between Primer and Propellant," Pts. I and II, AOA Paper, U.S. Army, Frankford Arsenal, Philadelphia, 1969.

[4] Kuo, K. K., Vichnevetsky, R., and Summerfield, M., "Theory of Flame Front Propagation in Porous Propellant Charges under Confinement," *AIAA Journal,* Vol. 11, April 1973, pp. 444-451.

[5] Bernecker, R. R. and Price, D., "Studies in the Transition from Deflagration to Detonation in Granular Explosives—I. Experimental Arrangement and Behavior of Explosives which Fail to Exhibit Detonation," *Combustion and Flame*, Vol. 22, Feb. 1974, pp. 111-118.

[6] Bernecker, R. R. and Price, D., "Studies in the Transition from Deflagration to Detonation in Granular Explosives—II. Transitional Characteristics and Mechanisms Observed in 91/9 RDX/WAX," *Combustion and Flame,* Vol. 22, Feb. 1974, pp. 119-129.

[7] Bernecker, R. R. and Price, D., "Studies in the Transition from Deflagration to Detonation in Granular Explosives—III. Proposed Mechanisms for Transition and Comparison with Other Proposals in the Literature," *Combustion and Flame*, Vol. 22, Apr. 1974, pp. 161-170.

[8] Warlick, G. L., "Ignition-Produced, Shock-Loading Phenomena in Naval Guns," CPIA Pub. 220, *8th JANNAF Combustion Meeting*, Vol. 1, Sept. 1971, pp. 71-81.

[9] Soper, W. G., "Grain Velocities During Ignition of Gun Propellant," *Combustion and Flame*, Vol. 24, April 1975, pp. 199-202.

[10] East, J. L. and McClure, D. R., "Experimental Studies of Ignition and Combustion in Naval Guns," *Proceedings 12th JANNAF Combustion Meeting,* Aug. 1975.

[11] Horst, A. W., "Solid Propellant Gun Interior Ballistics Annual Report: FY-75," Naval Ordnance Station, Indian Head, Md., IHTR 441, 1975.

[12] Horst, A. W., "Influence of Propellant Burning Rate Representation on Gun Environment Flame Spread and Pressure Wave Predictions," Naval Ordnance Station, Indian Head, Md. IHMR 76-255, 1976.

[13] Horst, A. W., Smith, T. C., and Mitchell, S. E., "Experimental Evaluation of Three Concepts for Reducing Pressure Wave Phenomena in Navy 5-Inch, 54 Caliber Guns: Summary of Firing Data," Naval Ordnance Station, Indian Head, Md., IHMR 76-258, 1976.

[14] Gerri, N. J., Pfaff, S. P., and Ortega, A. E., "Gas Flow in Porous Beds of Packed Propellant," Ballistic Research Laboratories, Aberdeen Proving Ground, Md., BRL IMR 159, 1973.

[15] Gerri, N. J. and Pfaff, S. P., "Gas Flow and Flame Spreading in a 20.16 cm Bed of Porous Propellant," Ballistic Research Laboratories, Aberdeen Proving Ground, Md., BRL IMR 420, 1975.

[16] Gerri, N. J., Stansbury, L., Jr., and Henry, C. L., "A Parametric Study of Gas Flow and Flame Spreading in Packed Beds of Ball Propellant. Part I. The 108.4 mm Chamber with 7.62 mm I.D." Ballistic Research Laboratories, Aberdeen Proving Ground, Md., BRL Rept. No. 1988, May 1977.

[17] Alkidas, A., Morris, S. O., Caveny, L. H., and Summerfield, M., "An Experimental Study of Pressure Wave Propagation in Granular Propellant Beds," *AIAA Journal*, Vol. 14, June 1976, pp. 789-792.

[18] Brosseau, T. L., "Development of the Minihat Pressure Transducer for Use in the Extreme Environments of Small Caliber Gun Barrels," Ballistic Research Laboratories, Aberdeen Proving Ground, BRL MR 2072, Nov. 1970.

[19] Stiefel, L. and Davis, R. M., "Burning Behavior of Several Typical Small Arms Propellants in Closed Bombs and in Guns," Frankford Arsenal, Philadelphia, MR M70-31-1, Sept. 1970.

[20] Kirshner, H. A. and Schlack, A. F., private communication, Frankford Arsenal, Oct. 1976.